

Cold or Warm? Constraining Dark Matter with Primeval Galaxies and Cosmic Reionization after Planck

A. Lapi^{a,b,c,d} L. Danese^{a,c,d}

^aSISSA, Via Bonomea 265, 34136 Trieste, Italy

^bDip. Fisica, Univ. ‘Tor Vergata’, Via Ricerca Scientifica 1, 00133 Roma, Italy

^cINAF-Osservatorio Astronomico di Trieste, Via Tiepolo 11, 34131 Trieste, Italy

^dINFN-Sezione di Trieste, Via Valerio 2, 34127 Trieste, Italy

E-mail: lapi@sissa.it, danese@sissa.it

Abstract. Dark matter constitutes the great majority of the matter content in the Universe, but its microscopic nature remains an intriguing mystery, with profound implications for particle physics, astrophysics and cosmology. Here we shed light on the longstanding issue of whether the dark matter is warm or cold by combining the measurements of the galaxy luminosity functions out to high redshifts $z \sim 10$ from the *Hubble Space Telescope* with the recent cosmological data on the reionization history of the Universe from the *Planck* mission. We derive robust and tight bounds on the mass of warm dark matter particle, finding that the current data require it to be in the narrow range between 2 and 3 keV. In addition, we show that a mass not exceeding 3 keV is also concurrently indicated by astrophysical constraints related to the local number of satellites in Milky Way-sized galaxies, though it is in marginal tension with analysis of the Lyman- α forest. For warm dark matter masses above 3 keV as well as for cold dark matter, to satisfy the *Planck* constraints on the optical depth and not to run into the satellite problem would require invoking astrophysical processes that inhibit galaxy formation in halos with mass $M_H \lesssim \text{few} \times 10^8 M_\odot$, corresponding to a limiting UV magnitude $M_{UV} \approx -11$. Anyway, we predict a downturn of the galaxy luminosity function at $z \sim 8$ faintward of $M_{UV} \approx -12$, and stress that its detailed shape is extremely informative both on particle physics and on the astrophysics of galaxy formation in small halos. These expectations will be tested via the *Hubble Frontier Fields* and with the advent of the *James Webb Space Telescope*, which will enable probing the very faint end of the galaxy luminosity function out to $z \sim 8 - 10$.

Keywords: dark matter theory — reionization — particle physics - cosmology connection

Contents

1	Introduction	1
2	Reionization history	3
3	Constraints on WDM particle mass	4
4	The astrophysicist’s view	6
5	Conclusions	8

1 Introduction

Several astrophysical and cosmological probes have firmly established that baryons — which stars, planets, and (known) living creatures are made of — constitute only some 15% of the total matter content in the Universe [1]. The rest is in the form of ‘dark matter’ (DM), which basically does not interact with the baryons except via long-range gravitational forces.

Still, no firm ‘direct’ identification of the DM particles has been made so far, although the progress in the sensitivity of detection experiments has been increasing dramatically over the past decade, and there are claims of intriguing, but not yet convincing, signals [2, 3]. Neither has robust evidence of DM been revealed from ‘indirect’ searches in the sky, by looking for γ -ray signals due to the annihilation or decay of DM particles at the Galactic center, in nearby galaxies, and in the diffuse γ -ray background [4–6]. The detection strategy that appears most promising today is the search for new physics in accelerators, and in particular at the *Large Hadron Collider* [7].

Thus the microscopic nature of the DM largely remains a mystery. Theoretically, based on extensions of the Standard Model, several candidate particles with different masses and properties have been proposed [8]; relevant examples are axions, sterile neutrinos, and weakly interacting massive particles (WIMPs) like the neutralino (the lightest supersymmetric particle). In particular, WIMPs with masses in the GeV range have long been considered a paradigm at the heart of the standard cosmological model. Such massive DM particles are ‘cold’ (hence the acronym CDM), i.e., non-relativistic at the epoch of their decoupling from the interacting particles in the Universe, and feature negligible free-streaming velocities from the initial perturbations of the cosmic density field.

CDM leads to a bottom-up structure formation, according to which bound DM structures called ‘halos’ grow hierarchically in mass and sequentially in time, with small clumps forming first and then stochastically merging together into larger and more massive objects [9]. These halos provide the gravitational potential wells where baryonic matter can settle in equilibrium, and via a number of complex astrophysical processes (e.g., cooling, star formation, energy feedback, etc.) originate the luminous structures that populate the visible Universe.

On large cosmological scales, data on galaxy clustering and on the cosmic microwave background confirm the above picture and are consistent with the CDM paradigm; recently, this has been tested to an unprecedented accuracy by the *Planck* mission [1]. However, on small scales the CDM paradigm has been challenged by at least two longstanding issues: the

cuspcore controversy, and the missing satellite problem. The former arises because N-body simulations predict the inner density profile of DM halos to be cuspy [10], whereas observations find them cored [11], i.e., round. The second problem comes because N-body simulations predict, for Milky Way-sized halos, the existence of a number of subhalos substantially larger than that of satellites found in our Galaxy [12].

On the one hand, it has been suggested that such issues can be alleviated within the standard CDM framework by accounting for the interplay between DM and baryons during the galaxy formation process [13–15]. On the other hand, they may also be solved by considering a different microscopic scenario for the DM particle; one appealing possibility is Warm Dark Matter (WDM) with masses in keV range, as provided by, e.g., a sterile neutrino. Being lighter than CDM, WDM particles remain relativistic for longer in the early universe and retain an appreciable residual velocity dispersion; so they more easily free-stream out from small-scale perturbations, suppressing the formation of subhalos and originating flat density distributions at the halo centers [16, 17]. The strength of these effects depends on the WDM particle mass; the lighter the particle mass M_{WDM} , the larger the free streaming scale $\propto M_{\text{WDM}}^{-1.15}$.

From an astrophysical perspective, the free streaming scales of the WDM particles can be indirectly probed by observations of the Lyman- α absorption produced by small clumps of neutral hydrogen in the spectra of distant quasars, the so called Lyman- α forest; lower bounds on the WDM mass $M_{\text{WDM}} \gtrsim 2 - 3$ keV have been derived [18, 19]. However, these analyses suffer from the uncertainties in the astrophysical modeling and numerical rendering of the intergalactic medium and of the intervening absorbers.

Here we exploit an alternative, direct probe of the WDM mass [20, 21], that is provided by the statistics of primeval galaxies observed out to $z \sim 10$, supplemented with the data on the reionization history of the Universe from cosmological observations; we recall that reionization is the process by which the intergalactic medium has transitioned again to an ionized state (it was already fully ionized before the epoch of recombination, when the Universe was younger than 380.000 yr) due to the radiation from the first astrophysical sources.

In a nutshell, the argument runs as follows. Faint galaxies at $z \gtrsim 4$ are the main responsible for the cosmic reionization (although faint active galactic nuclei may also contribute [22, 23]¹), whose history has been recently constrained by the *Planck* mission [1] in terms of integrated optical depth $\tau_{\text{es}} \approx 0.066 \pm 0.012$ for Thomson scattering to the cosmic microwave background². This measurement gauges the level of the ionizing background from primeval galaxies, and in turn (although with some assumptions to be discussed next) their number density. These galaxies reside in small halos, so that their number density can provide a direct test of the WDM free-streaming scale, and sets bounds on the particle mass.

Our working plan is straightforward: in Section 2 we present the reionization history of the Universe as inferred from high-redshift galaxy statistics and cosmological data; in Section 3 we derive the related constraints on the WDM particle mass; in Section 4 we discuss

¹Given their number density much smaller than protogalaxies’ (see also [24]), AGN-driven reionization requires an escape fraction $f_{\text{esc}} \approx 1$.

²The analysis of only *Planck* data (TT, TE, EE spectra + low- ℓ polarization + lensing) yields $\tau_{\text{es}} \approx 0.063 \pm 0.014$, while when external data (e.g., BAOs) are added, the value quoted in the main text is found. We stress that in the Λ CDM cosmology, τ_{es} is appreciably degenerate with the amplitude A_s of the primordial perturbation spectrum, but the associated variations are still within its 2σ uncertainty; finally, τ_{es} is essentially unaffected in minimal extensions of the standard Λ CDM model by the effective neutrino number N_{eff} , by dynamical dark energy w_Λ , etc.

the connection between the microscopic nature of DM and the macroscopic, astrophysical properties of galactic halos; in Section 5 we summarize our findings.

Throughout the work we adopt the standard, flat cosmology [1] with matter density parameter $\Omega_M = 0.31$, baryon density parameter $\Omega_b = 0.05$, Hubble constant $H_0 = 100 h$ km s⁻¹ Mpc⁻¹ with $h = 0.68$, and mass variance $\sigma_8 = 0.81$.

2 Reionization history

Our starting point is constituted by the UV luminosity function of galaxies at redshift $z \gtrsim 4$, illustrated in Fig. 1. Circles refer to data points from observations with the *Hubble Space Telescope* [25] (see also [26]), while the solid lines are their analytic renditions in terms of continuous Schechter functions $dN/dM_{UV} \propto 10^{-0.4(M_{UV}-M_{UV}^*)(\alpha+1)} \times \exp[-10^{-0.4(M_{UV}-M_{UV}^*)}]$; these feature a faint-end powerlaw slope α steepening from -1.7 to -2.3 as z increases from 4 to 10, and an exponential cutoff brightward of a characteristic magnitude M_{UV}^* correspondingly ranging from -21.5 to -20.5 . We recall that the UV magnitude and luminosity are related by $M_{UV} \approx 5.9 - 2.5 \log \nu L_{UV}[L_\odot]$, where ν is the frequency corresponding to 1550 Angstroms, and $L_\odot \approx 3.8 \times 10^{33}$ erg s⁻¹ is the bolometric solar luminosity.

The dashed lines illustrate the outcomes after correction for dust extinction estimated from the UV continuum slope [27]. Dust correction is irrelevant for magnitudes fainter than $M_{UV} \approx -17$, but it is useful to provide an estimate of the intrinsic star formation rate (SFR) in primeval galaxies. The relation between UV magnitude and SFR depends on the initial mass function (IMF), i.e., on the distribution of stellar masses formed per unit SFR. For the locally observed Chabrier [28] IMF, the relation $M_{UV} \approx 18.5 - 2.5 \log \text{SFR}[M_\odot \text{ yr}^{-1}]$ holds, and has been used in labeling the upper scale of Fig. 1.

Based on the observed luminosity functions (without dust-correction), we then compute the reionization history of the Universe, in terms of the evolution with redshift of the electron scattering optical depth τ_{es} . In brief, this is performed as follows. Firstly, the ionization rate

$$\dot{N}_{\text{ion}} \approx f_{\text{esc}} k_{\text{ion}} \int^{M_{UV}^{\text{lim}}} dM_{UV} \frac{dN}{dM_{UV}} L_{UV} \quad (2.1)$$

is found on multiplying the integral of the UV luminosity functions down to a limiting UV magnitude M_{UV}^{lim} by the number $k_{\text{ion}} \approx 2 \times 10^{56}$ of ionizing photons yr⁻¹ L_\odot^{-1} as appropriate for a Chabrier IMF, and again by the average escape fraction $f_{\text{esc}} \approx 0.2$ of ionizing photons from the interstellar medium of primeval galaxies [29–31]. Then, the ionization rate is inserted into the standard evolution equation of the HII ionizing fraction

$$\dot{Q}_{\text{HII}} = \frac{\dot{N}_{\text{ion}}}{\bar{n}_{\text{H}}} - \frac{Q_{\text{HII}}}{t_{\text{rec}}} \quad (2.2)$$

that takes into account the competition between ionization and recombination processes [32, 33]. In the above equation $\bar{n}_{\text{H}} \approx 2 \times 10^{-7} (\Omega_b h^2 / 0.022) \text{ cm}^{-3}$ is the mean comoving hydrogen number density. In addition, the recombination timescale reads $t_{\text{rec}} \approx 3.2 \text{ Gyr} [(1+z)/7]^{-3} C_{\text{HII}}^{-1}$, where the case B coefficient for an IGM temperature of 2×10^4 K has been used; this timescale crucially depends on the clumping factor of the ionized hydrogen, for which a fiducial value $C_{\text{HII}} \approx 3$ is adopted [34]. We shall discuss later the dependence of our results on these parameters. Finally, the electron scattering optical depth is obtained by integrating the ionized fraction over redshift

$$\tau_{\text{es}}(z) = c \sigma_{\text{T}} \bar{n}_{\text{H}} \int^z dz' f_e Q_{\text{HII}}(z') (1+z')^2 H^{-1}(z') ; \quad (2.3)$$

here $H(z) = H_0 [\Omega_M (1+z)^3 + 1 - \Omega_M]^{1/2}$ is the Hubble parameter, c is the speed of light, σ_T the Thomson cross section and f_e the number of free-electron (computed assuming double Helium ionization at $z \lesssim 4$).

The outcome is illustrated in Fig. 2 for three representative values of the limiting UV magnitude at the faint end: red lines are for $M_{UV} \lesssim -17$, green lines refer to $M_{UV} \lesssim -13$ and blue lines to $M_{UV} \lesssim -11$; these produce integrated optical depths τ_{es} covering the 1σ region measured by *Planck*, with the value $M_{UV}^{\text{lim}} \approx -13$ approximately yielding the *Planck* best fit $\tau_{es} \approx 0.066$ [35] (to be precise, we obtain asymptotically $\tau_{es} \approx 0.06$, while we find $\tau_{es} \approx 0.055$ if truncating the cosmic SFR at $z \gtrsim 8-10$, cf. [31]). For reference, the dotted line represents the optical depth expected in a fully ionized Universe up to redshift z ; this is to show that the bulk of the reionization process occurred at $z \sim 8-10$ and was almost completed at $z \sim 6$ [36]. Note that from this perspective, the detailed behavior of the luminosity functions at $z \gtrsim 10$ (that have been computed by extrapolation of the lower-redshift behavior), and the related ionizing background, are only marginally relevant. This is also apparent from the inset of Fig. 2, where the evolution with redshift of the ionizing fraction Q_{HII} is illustrated, and confronted with various observational constraints [31].

We note that the range $M_{UV} \lesssim -17$ roughly corresponds to the luminosity function currently observed at $z \sim 4-8$ and already yields $\tau_{es} \approx 0.045$. Going fainter to reproduce the *Planck* best-fit value or the 1σ upper bound requires instead an extrapolation into magnitude ranges currently inaccessible to observations at these redshifts. One may wonder whether these extrapolations down to fainter luminosities are reasonable. Actually, at lower redshift $z \sim 2$ the faint end of the luminosity function has been explored down to $M_{UV} \approx -13$ thanks to gravitational lensing by a foreground galaxy cluster [37]; the data, illustrated by the magenta stars in Fig. 1, indicates that the faint portion of the luminosity function keeps rising, similarly to what happens with our extrapolations at higher z .

3 Constraints on WDM particle mass

We now aim at confronting the luminosity function of primeval galaxies with the number density of the host DM halos. In Fig. 3 we illustrate the mass function of halos $dN/d \log M_H$ at the relevant redshift $z \sim 8$ where the bulk of the reionization process occurs. We compute this quantity based on analytic expressions for the halo mass function from the excursion set theory [38, 39], that approximate very well the outcomes of N -body simulations for CDM [40]; for the WDM cases, we compute the mass variance (that enters the excursion set mass function) by adopting a sharp filter in k -space, calibrated as prescribed by [42, 43] to reproduce the outcomes of WDM simulations at different redshifts [43–45].

In Fig. 3 the solid black line refers to the CDM case, while the colored lines show the outcomes for different WDM masses $M_{\text{WDM}} = 1, 2, 3$ keV. For WDM the halo mass function is depressed below the free streaming mass of the particles, that amounts to about $10^8 M_\odot$ for $M_{\text{WDM}} \approx 2$ keV and roughly scales as $M_{\text{WDM}}^{-3.5}$. Note that we quote here the Fermi–Dirac mass, i.e., the mass that the WDM particles would have if they were thermal relics (decoupled in thermal equilibrium); this is convenient because the masses of WDM particles produced in different microscopic scenarios can be easily related to this quantity [41].

We should mention that the behavior of the halo mass function below the free-streaming mass is somewhat debated, with various simulations and analytic approaches providing quite different results [42, 43, 45], especially at high redshifts $z \gtrsim 3$. In particular, the effective pressure from the residual WDM velocity dispersion can make the truncation at small masses

more dramatic; the dotted colored lines in Fig. 3 are empirical renditions of these more extreme behaviors [46].

Now we come to the key point. In Fig. 4 we present the integrated number density of DM halos $N(> \log M_{\text{H}})$ with mass larger than M_{H} at the relevant redshift $z \sim 8$. This is to be compared with the integrated number density of faint galaxies down to the three limits $M_{\text{UV}}^{\text{lim}} \approx -17, -13, -11$ relevant for reionization (cf. Fig. 2), which are illustrated by the labeled grey shaded areas. This comparison highlights that for small WDM particle masses, the number density in halos simply does not attain the levels implied by the galaxy luminosity functions. Specifically, it is evident that the observed galaxy number density down to $M_{\text{UV}} \approx -17$ straightforwardly constrains the WDM particle masses to be $M_{\text{WDM}} \gtrsim 1$ keV; values lower than this limit are ruled out, essentially in a model-independent way. In fact, comparison between the solid and dotted lines highlights that the uncertainty in the behavior of the halo mass function below the free-streaming mass scale does not affect our conclusion.

Moreover, as discussed above, the reionization history of the Universe implied by the recent *Planck* data for τ_{es} requires the luminosity function to be extrapolated at least up to $z \sim 10$ with a steep slope $\alpha \approx -2$ down to $M_{\text{UV}} \approx -13$, strengthening the constraints on the WDM mass to $M_{\text{WDM}} \gtrsim 2$ keV. On the other hand, consistency with the *Planck* 1σ upper limit on τ_{es} requires the luminosity function not to rise by much beyond $M_{\text{UV}} \approx -11$, implying the upper bound $M_{\text{WDM}} \lesssim 3$ keV.

We stress that such constraints are direct and robust, since they only require minimal assumptions. Specifically, in Fig. 5 we show how the UV limiting magnitude and the associated number density of galaxies required to match the *Planck* best fit value on $\tau_{\text{es}} \approx 0.066$, change with the relevant parameters, namely, the IMF (via k_{ion} in Eq. 2.1), the escape fraction f_{esc} of ionizing photons, the slope α of the faint-end luminosity function and the clumping factor C_{HII} of the intergalactic medium. The fiducial values are highlighted as cyan stars, while higher or lower values are marked by labeled circles. Moving upward in the plot from the fiducial value implies fainter magnitudes and higher galaxy number density, hence tighter constraints on the WDM mass, and viceversa. Note that here the parameters are varied one by one while the others are kept fixed. However, their degeneracy in producing a given reionization history can be highlighted by the approximate expression $f_{\text{esc}} k_{\text{ion}} C_{\text{HII}}^{-0.3} \Gamma[\alpha + 2; 10^{-0.4(M_{\text{UV}}^{\text{lim}} - M_{\text{UV}}^*)}] \approx \text{const}$ (cf. also Eq. 6 in [35]), where $\Gamma[a; z] \equiv \int_z^\infty dx x^{a-1} e^{-x}$ is the incomplete Γ -function; the most important dependencies are on f_{esc} and on the limiting magnitude $M_{\text{UV}}^{\text{lim}}$, given the noticeable observational uncertainties on these parameters.

In more detail, switching from a Chabrier to a Salpeter IMF [47] implies fewer ionizing photons being produced for a given SFR (parameter k_{ion}), hence the limiting magnitude required to reproduce the *Planck* data increases from $M_{\text{UV}} \approx -12.5$ to ≈ -11 , the corresponding galaxy number density rises from $N(> \log M_{\text{H}}) \approx -0.5$ to $\approx +0.5$, and the lower bounds on the WDM mass strengthen from $M_{\text{WDM}} \gtrsim 2$ keV to $\gtrsim 3$ keV, cf. Fig. 4. Conversely, switching from the observed Chabrier IMF to a hypothetical top-heavy IMF [48] enhances the number of ionizing photons, and causes the limiting magnitude to change from $M_{\text{UV}} \approx -12.5$ to ≈ -15.5 , the number density to decrease from $N(> \log M_{\text{H}}) \approx -0.5$ to ≈ -1.75 , and the lower bounds on the WDM mass to weaken from $M_{\text{WDM}} \gtrsim 2$ keV to $\gtrsim 1.25$ keV; however, note that such a top-heavy IMF would imply a correspondingly stronger metal and dust enrichment of the interstellar medium in primeval galaxies already at $z \sim 8$, which is not expected for these faint UV sources and in turn would dramatically reduce their ionization efficiency.

For the other parameters: the clumping factor of the intergalactic medium has a small

impact on our results, while the escape fraction and the faint-end slope of the luminosity function are more critical. Specifically, increasing the escape fraction from the fiducial value of 0.2 to 0.4 or steepening the slope of the luminosity function from the fiducial $\alpha \approx -2$ to -2.25 would shift the allowed range of the WDM mass to $1.5 \lesssim M_{\text{WDM}}/\text{keV} \lesssim 2.5$ keV.

However, values of $f_{\text{esc}} \approx 0.2$ are considered conservative upper limits, actually attained only for faint galaxies at high redshift $z \gtrsim 3$; this is demonstrated both by refined estimates [49–51] of the ionizing emissivity from galaxies out to $z \sim 4$ and by observations in local analogs of high- z faint galaxies [52]. Note that some recent hydrodynamical simulations [53, 54] aimed at studying protogalaxies suggest a slight increase of the escape fraction with decreasing halo mass, due to a combination of supernova feedback efficiency and dense gas column density, but still produce values limited to $f_{\text{esc}} \lesssim 0.2$ in the range of low mass halos $M_{\text{H}} \lesssim 10^9 M_{\odot}$ relevant for reionization (see Section 4).

Concerning the slope of the luminosity function, the current data at $z \sim 8$, limited to $M_{\text{UV}} \lesssim -17$, indicates values close to our fiducial $\alpha \approx -2$. Similar if slightly shallower slopes have been found at lower $z \sim 4-6$ in the same magnitude range (cf. Fig. 1); moreover, values of $\alpha \approx -1.8$ are measured at $z \sim 2$ from the ultra-faint data [37] that probes the luminosity function down to $M_{\text{UV}} \approx -13$. A slope of $\alpha \approx -1.8$ instead of -2 at $z \sim 8$ would imply a lower bound on the WDM mass of $M_{\text{WDM}} \gtrsim 5$ keV. In the near future, a closer assessment of the faint-end slope will become available via the *Hubble Frontier Fields* Program (see <http://www.stsci.edu/hst/campaigns/frontier-fields/>), and with the advent of the James Webb Space Telescope [55], which will allow probing the galaxy luminosity function at $z \sim 8-10$ down to magnitudes $M_{\text{UV}} \approx -13$, and potentially even fainter by taking advantage of gravitational lensing effects [56].

4 The astrophysicist’s view

As a final step, we now turn to connecting the microscopic nature of the DM with the macroscopic astrophysical properties of primeval galaxies. For doing this, we aim at deriving an average statistical relationship between the UV magnitude of a galaxy (or the SFR) and its host halo mass; this can be done via the abundance matching technique [57–59], i.e., by associating galaxies and halos with the same integrated number density. The outcome at the relevant redshift $z \sim 8$ is illustrated in Fig. 6, both for CDM and three representative values of the WDM mass. Comparisons between the solid and dashed/dotted lines highlight that the outcome is insensitive to dust-corrections in the luminosity functions and/or to the behavior of the WDM mass function below the free-streaming mass length.

We find a relationship $\text{SFR} \propto M_{\text{H}}^{1.45}$ between the SFR and host halo mass, which is remarkably similar to what has been derived in the higher mass range $10^{11} \lesssim M_{\text{H}}/M_{\odot} \lesssim 10^{12}$ at lower $z \lesssim 6$ [60]; the slope is close to that expected for galaxies where the SFR is regulated by the balance between cooling and energy feedback from supernova explosions or stellar winds [61]. In WDM scenarios, the power-law relationship somewhat flattens and then stops at around the free-streaming mass scale, just because low mass halos are not formed, while it would extend down to very small halos in a CDM Universe.

As shown by numerical simulations [63], this is actually a serious issue for CDM, because a substantial number of such small halos would survive down to the present time as bound satellites of Milky Way-sized galaxies, which are not observed. This is another way of presenting the missing satellite problem mentioned at the beginning of this article. Solving the issue for CDM requires invoking astrophysical processes that must severely limit or even

suppress galaxy formation in halos with masses $M_{\text{H}} \lesssim \text{few} \times 10^8 M_{\odot}$ (cf. the yellow-shaded area in Fig. 6), corresponding to UV magnitudes fainter than $M_{\text{UV}} \approx -11$ at $z \sim 8$; remarkably, this is the same limit concurrently indicated by the 1σ upper bound on τ_{es} from the *Planck* data. We stress that the limiting magnitude $M_{\text{UV}} \approx -11$ imposed by the satellite problem is independent on f_{esc} ; once this limit is respected, then f_{esc} cannot be much different from 0.2 to yield the *Planck* value of $\tau_{\text{es}} \approx 0.066$. Physical processes suppressing galaxy formation may include an increase of supernova feedback efficiency in such small halos, or radiative feedback from the diffuse UV background, or more complex phenomena [64–66]. On the other hand, the satellite issue is naturally solved in WDM with $M_{\text{WDM}} \lesssim 3 \text{ keV}$ since halos with $M_{\text{H}} \lesssim \text{few} \times 10^8 M_{\odot}$ are not formed at all, and even cooling/star formation processes may be less efficient due to the lack of substructures [15].

We remark that the combination of these astrophysical constraints on the satellite problem with the cosmological data on reionization further restrict the plausible range of parameter values investigated in Fig. 5. For example, a very low value of the escape fraction $f_{\text{esc}} \approx 0.05$ as sometimes claimed in literature [53] would require the reionization process to be triggered at $z \gtrsim 10$ by very faint galaxies with $M_{\text{UV}} \approx -8$. This in turn would imply the WDM mass to exceed 5 keVs and hence to be indistinguishable from CDM. On the other hand, such very faint galaxies residing in halo masses $M_{\text{H}} \lesssim 10^8 M_{\odot}$ would largely exceed the observed number of local satellites.

We recall from Fig. 2 that the primeval galaxies contributing most to the cosmic reionization have UV magnitudes $M_{\text{UV}} \approx -13$; in turn, from Fig. 6, these are seen to be hosted in halos with $M_{\text{H}} \approx 10^9 M_{\odot}$ and to feature typical $\text{SFR} \approx 10^{-2} M_{\odot} \text{ yr}^{-1}$. The reionization process started at $z \sim 10$ and nearly completed at $z \sim 6$, corresponding to a relatively short time lapse of a few $\times 10^8 \text{ yr}$. Thus the typical stellar masses accumulated in the primeval galaxies responsible for reionization are $M_{\star} \approx \text{few} \times 10^6 M_{\odot}$. Remarkably, this is consistent with the extrapolation down to $M_{\text{UV}} \approx -13$ of the M_{\star} vs. M_{UV} relationship [67] currently estimated at $z \sim 7$ for $M_{\text{UV}} \lesssim -18$. The corresponding stellar mass density at $z \sim 8$ amounts to $\approx 10^6 M_{\odot} \text{ Mpc}^{-3}$, which turns out to be 1/300 of the integrated local value at $z \sim 0$. We note that the relative narrow redshift range of the reionization between $z \sim 10$ and $z \sim 6$ as inferred from the *Planck* data will ease tomographic mapping of the HI distribution via the redshifted 21 cm line with the *Square Kilometer Array* [68, 69].

In Fig. 7 we provide specific predictions on the very faint end of the UV luminosity function at $z \sim 8$, obtained by combining the M_{UV} vs. M_{H} relationships of Fig. 6 with the halo mass function of Fig. 3; note that the faint-end slope of the luminosity function mirrors that of the halo mass function [25]. We check that for magnitudes $M_{\text{UV}} \lesssim -17$ the input luminosity function based on *Hubble Space Telescope* data by [25] is recovered; moreover, at the very faint end currently precluded to observations, we can predict the behavior of the luminosity function. Specifically, for WDM masses M_{WDM} in the relevant range from 2 to 3 keVs, we expect an abrupt downturn of the luminosity function at magnitudes M_{UV} in the range from -13 to -11 basically due to the lack of substructures.

On the other hand, for pure CDM the luminosity function would continue to rise steeply, infringing the *Planck* constraints on τ_{es} if $M_{\text{UV}} \gtrsim -11$. However, as we have discussed above, baryonic processes must also intervene not to run into the satellite problem; these will flatten the luminosity function for halo masses $M_{\text{H}} \lesssim \text{few} \times 10^8 M_{\odot}$, corresponding (cf. Fig. 6) to UV magnitudes $M_{\text{UV}} \approx -12$. In this case the flattening is expected to be more gentle because of the variance associated to the underlying astrophysical processes, as represented by the dashed line in Fig. 7.

Again we stress that the reionization history of the Universe (cf. Fig. 2) inferred from the *Planck* data [1] on τ_{es} and the missing satellite problem (cf. Fig. 6) *concurrently* indicate that the luminosity function must downturn in the range of magnitudes $-13 \lesssim M_{\text{UV}} \lesssim -11$. In all these respects, the location and the detailed shape of the luminosity function near the downturn would be extremely informative both on particle physics and on the astrophysics of galaxy formation in small halos [62]. Whatever is its origin, DM nature or baryon astrophysics, the downturn of the luminosity function is expected to occur not far from the magnitudes that has been already observed at $z \sim 2$ [37] thanks to gravitational lensing effects. At $z \sim 8$ the relevant magnitude range will be probed in the next future via the *Hubble Frontier Fields* and with the advent of the *James Webb Space Telescope*.

5 Conclusions

In summary, we have shown that accurate observations on the number density of primeval galaxies (cf. Fig. 1), supplemented with cosmological data constraining the history of cosmic reionization (cf. Fig. 2), have a strong potential for unveiling the elusive nature of dark matter. Specifically, we have obtained a robust lower bound $M_{\text{WDM}} \gtrsim 1$ keV from the number density of primeval galaxies currently observed down to $M_{\text{UV}} \approx -17$ at $z \lesssim 8$ (cf. Figs. 3 and 4). In addition, the *Planck* measurements on the electron scattering optical depth $\tau_{\text{es}} \approx 0.066$ (and constraints on the evolution of the ionized fraction from various astrophysical probes) can be reproduced with standard, observationally supported (at least for $z \lesssim 3$) assumptions on the escape fraction $f_{\text{esc}} \approx 0.2$, the clumping factor $C_{\text{HII}} \approx 3$, and the faint-end slope $\alpha \approx -2$ of the luminosity function extrapolated down to the UV limiting magnitude $M_{\text{UV}} \approx -13$.

Such values imply an even tighter constraint on the WDM mass $M_{\text{WDM}} \gtrsim 2$ keV; on the other hand, an upper bound $M_{\text{WDM}} \lesssim 3$ keV is concurrently indicated by the 1σ upper limit on the *Planck* data on τ_{es} and by astrophysical constraints related to the local number of satellites in Milky Way-sized galaxies (cf. Fig. 6), though it is in marginal tension with analysis of the Lyman- α forest (see also discussion by [70]). This shows that, in the perspective of astrophysics and cosmology, only WDM endowed with particle masses just around $2 - 3$ keV is a relevant alternative to the CDM case. On the other hand, for WDM masses above 3 keV as well as for CDM, to comply with the *Planck* constraints on τ_{es} and not to run into the satellite problem would require invoking astrophysical processes that inhibit galaxy formation in halos with mass $M_{\text{H}} \lesssim \text{few} \times 10^8 M_{\odot}$, corresponding to $M_{\text{UV}} \approx -11$.

As a specific prediction, we expect a downturn of the galaxy luminosity function at $z \sim 8$ faintward of $M_{\text{UV}} \approx -12$, which should be more abrupt if it is due to the free-streaming scale associated with WDM, or more progressive if due to astrophysical processes in a CDM Universe (cf. Fig. 7). Such a downturn is expected to occur not far from the magnitudes that has been already observed at $z \sim 2$ [37] thanks to gravitational lensing effects. These expectations will be tested via the *Hubble Frontier Fields* and with the advent of the *James Webb Space Telescope*, which will enable probing the very faint end of the galaxy luminosity function out to $z \sim 8 - 10$. Specifically, its detailed shape will eventually answer the question: which is the main cause regulating galaxy formation within small galaxy halos, particle physics or astrophysics?

Acknowledgments

This work has been supported in part by the MIUR PRIN 2010/2011 ‘The dark Universe and the cosmic evolution of baryons: from current surveys to Euclid’, by the INAF PRIN 2012/2013 ‘Looking into the dust-obscured phase of galaxy formation through cosmic zoom lenses in the Herschel Astrophysical Terahertz Large Area Survey’. We acknowledge our referee for helpful comments. We are grateful to R. Aversa, A. Cavaliere, C. Baccigalupi, G. De Zotti, P. Salucci, and A. Schneider for discussions, and to J. Miller for critical reading. A.L. thanks SISSA for warm hospitality.

References

- [1] Planck Collaboration, *Planck 2015 results, XIII, Cosmological parameters*, A&A submitted (2015), arXiv:150201589.
- [2] Bertone, G., Hooper, D., Silk, J., *Particle dark matter: evidence, candidates and constraints*, PhR **405** (2004), 279
- [3] Feng, J.L., *Dark Matter Candidates from Particle Physics and Methods of Detection*, ARAA **48** (2010), 495
- [4] Ackermann, M., et al., *Constraints on the Galactic Halo Dark Matter from Fermi-LAT Diffuse Measurements*, ApJ **761** (2012), 91
- [5] Ackermann, M., et al., *Dark matter constraints from observations of 25 Milky-Way satellite galaxies with the Fermi Large Area Telescope*, PhRvD **89** (2014), 2001
- [6] The Fermi LAT Collaboration, *Limits on dark matter annihilation signals from the Fermi LAT 4-year measurements of the isotropic gamma-ray background*, JCAP, submitted (2015), arXiv:150105464.
- [7] Mitsou, V.A., *Overview of searches for dark matter searches at the LHC*, J. Phys. Conf. Ser., in press (2015), arXiv:1402.3673
- [8] Bertone, G., *The moment of truth for WIMP dark matter*, Nature **468** (2010), 389.
- [9] Frenk, C.S., White, S.D.M., *Dark matter and cosmic structure*, Annalen der Physik **524** (2012), 507
- [10] J. F. Navarro, C. S. Frenk, and S. D. M. White, *A Universal Density Profile from Hierarchical Clustering*, ApJ **490** (1997) 493
- [11] Salucci, P., Wilkinson, M.I., Walker, M.G., Gilmore, G.F., Grebel, E.K., Koch, A., Frigerio Martins, C., Wyse, R.F.G., *Dwarf spheroidal galaxy kinematics and spiral galaxy scaling laws*, MNRAS **420** (2012), 2034.
- [12] Boylan-Kolchin, M., Bullock, J.S., Kaplinghat, M., *The Milky Way’s bright satellites as an apparent failure of LambdaCDM*, MNRAS **422** (2012), 1203.
- [13] El-Zant, A., Shlosman, I., Hoffman, Y., *Dark Halos: the flattening of the density cusp by dynamical friction*, ApJ **560** (2001), 636
- [14] Tonini, C., Lapi, A., Salucci, P., *Angular Momentum Transfer in Dark Matter Halos: Erasing the Cusp*, ApJ **649** (2006), 591
- [15] Pontzen, A., Governato, F., *Cold dark matter heats up*, Nature **506** (2014), 171
- [16] P. Bode, J. P. Ostriker, and N. Turok, *Halo Formation in Warm Dark Matter Models*, ApJ **556** (2001) 93
- [17] Lovell, M.R., et al., *The properties of warm dark matter haloes*, MNRAS **439** (2014), 300

- [18] Seljak, U., Makarov, A., McDonald, P., and Trac, H., *Can Sterile Neutrinos Be the Dark Matter?*, Phys. Rev. Lett. **97** (2006), 1303
- [19] Viel, M., Becker, G., Bolton, J.S., Haehnelt, M.G., *Warm dark matter as a solution to the small scale crisis: New constraints from high redshift Lyman-alpha forest data*, PhRvD **88** (2013), 3502
- [20] Pacucci, F., Mesinger, A., Haiman, Z., *Focusing on warm dark matter with lensed high-redshift galaxies*, MNRAS, **435** (2013), L53
- [21] Schultz, C., Oñorbe, J., Abazajian, K.N., Bullock, J.S., *The high- z universe confronts warm dark matter: Galaxy counts, reionization and the nature of dark matter*, MNRAS **442** (2014), 1597
- [22] Giallongo, E., et al., *Faint AGNs at $z > 4$ in the CANDELS GOODS-S field: looking for contributors to the reionization of the Universe*, A&A in press (2015), arXiv:1502.02562
- [23] Madau, P., and Haardt, F., *Cosmic Reionization after Planck: Could Quasars Do It All?*, ApJ submitted (2015), arXiv:150707678
- [24] Weigel, A.K., Schawinski, K., Treister, E., Urry, C. M., Koss, M., and Trakhtenbrot, B., *The systematic search for $z > 5$ active galactic nuclei in the Chandra Deep Field South*, MNRAS **448**, 3167
- [25] Bouwens, R.J., Illingworth, G.D., Oesch, P.A., *UV Luminosity Functions at redshifts $z \sim 4$ to $z \sim 10$: 11000 Galaxies from HST Legacy Fields*, ApJ **803** (2015), 34
- [26] McLeod, D. J., et al., *New redshift $z \sim 9$ galaxies in the Hubble Frontier Fields: Implications for early evolution of the UV luminosity density*, MNRAS **450** (2015), 3032
- [27] Bouwens, R.J., Illingworth, G.D., Oesch, P.A., *UV-continuum slopes of $\sim 4000 z \sim 4 - 8$ galaxies from the HUDF/XDF, HUDF09, ERS, CANDELS-South, and CANDELS-North fields*, ApJ **793** (2014), 115
- [28] Chabrier, G., *Galactic Stellar and Substellar Initial Mass Function*, PASP **115** (2003), 763
- [29] Mao, J., Lapi, A., Granato, G. L., de Zotti, G., and Danese, L., *The Role of the Dust in Primeval Galaxies: A Simple Physical Model for Lyman Break Galaxies and Ly- α Emitters*, ApJ **667**, 655
- [30] Dunlop, J.S., et al., *The UV continua and inferred stellar populations of galaxies at $z \sim 7 - 9$ revealed by the Hubble Ultra-Deep Field 2012 campaign*, MNRAS **432** (2013), 3520
- [31] Robertson, B.E., Ellis, R.S., Furlanetto, S.R., Dunlop, J.S., *Cosmic reionization and early star-forming galaxies: a joint analysis of new constraints from Planck and Hubble Space Telescope*, ApJ, **802** (2015), L19
- [32] Madau, P., Haardt, F., Rees, M.J., *Radiative transfer in a clumpy Universe. III. The nature of cosmological ionizing sources*, ApJ **514** (1999), 648
- [33] Ferrara, A., Pandolfi, S., *Reionization of the Intergalactic Medium*, in ‘New Horizons for Observational Cosmology’, eds. A. Melchiorri, A. Cooray, E. Komatsu, (2015, Bologna: SIF press), in press, arXiv:1409.4946
- [34] Pawlik, A.H., Milosavljevic, M., Bromm, V., *The First Galaxies: Assembly under Radiative Feedback from the First Stars*, ApJ **767** (2013), 59
- [35] Bouwens, R. J., et al., *Cosmic Reionization after Planck: The Derived Growth of the Ionizing Background now matches the Growth of the Galaxy UV Luminosity Density*, ApJ, submitted (2015), arXiv:150308228
- [36] Shull, J. M., Harness, A., Trenti, M., Smith, B. D., *Critical Star Formation Rates for Reionization: Full Reionization Occurs at Redshift $z \sim 7$* , ApJ **747**, 100

- [37] Alavi, A., et al., *Ultra-faint Ultraviolet Galaxies at $z \sim 2$ behind the Lensing Cluster A1689: The Luminosity Function, Dust Extinction, and Star Formation Rate Density*, ApJ **780** (2014), 143
- [38] Sheth, R.K., Mo, H.J., Tormen, G., *Ellipsoidal collapse and an improved model for the number and spatial distribution of dark matter haloes*, MNRAS **323** (2001), 1
- [39] Lapi, A., Salucci, P., Danese, L., *Statistics of dark matter halos from the excursion set approach*, ApJ **772** (2013) 85
- [40] Tinker, J.L., et al., *Toward a halo mass function for precision cosmology: The Limits of universality*, ApJ **688** (2008), 709
- [41] Kusenko, A., *Sterile neutrinos: the dark side of the light fermions*, PhR **481** (2009), 1
- [42] Benson, A.J., et al., *Dark matter halo merger histories beyond cold dark matter - I. Methods and application to warm dark matter*, MNRAS **428** (2013), 1774
- [43] Schneider, A., Smith, R.E., Reed, D., *Halo mass function and the free streaming scale*, MNRAS **433** (2013), 1573
- [44] Angulo, R.E., Hahn, O., and Abel, T., *The warm dark matter halo mass function below the cut-off scale*, MNRAS **434** (2013), 3337
- [45] Bose, S., et al., *The COpernicus COmplexio: Statistical Properties of Warm Dark Matter Haloes*, MNRAS submitted (2015), arXiv:1507.01998
- [46] Smith, R. E., Markovic, K., *Testing the warm dark matter paradigm with large-scale structures*, Phys. Rev. D **84** (2011), 3507
- [47] Salpeter, E.E., *The Luminosity Function and Stellar Evolution*, ApJ **121** (1955), 161
- [48] Greggio, L., Renzini, A., *Stellar Populations: a User Guide from Low to High Redshift* (2011, Wiley-VCH Verlag), ISBN 978-3-527-40918-1
- [49] Nestor, D.B., Shapley, A.E., Kornei, K.A., Steidel, C.C., Siana, B., *A Refined Estimate of the Ionizing Emissivity from Galaxies at $z \sim 3$: Spectroscopic Follow-up in the SSA22a Field*, ApJ **765** (2013), 47
- [50] Cooke, J., Ryan-Weber, E. V., Garel, T., Díaz, C. G., *Lyman-continuum galaxies and the escape fraction of Lyman-break galaxies*, MNRAS **441** (2014), 837
- [51] Vanzella, E., et al., *Peering through the holes: the far-UV color of star-forming galaxies at $z \sim 3-4$ and the escaping fraction of ionizing radiation*, A&A **576** (2015), 116
- [52] Borthakur, S., Heckman, T.M., Leitherer, C., Overzier, *A local clue to the reionization of the universe*, Science **246** (2014), 216
- [53] Ma, X., et al., *The Difficulty Getting High Escape Fractions of Ionizing Photons from High-redshift Galaxies: a View from the FIRE Cosmological Simulations*, MNRAS submitted, arXiv:150307880
- [54] Paardekooper, J.-P., Khochfar, S., Dalla Vecchia, C., *The First Billion Years project: the escape fraction of ionizing photons in the epoch of reionization*, MNRAS, **451** (2015), 2544
- [55] Gardner, J.P., et al., *The James Webb Space Telescope*, Sp. Sci. Rev. **123** (2006), 485
- [56] Atek, H., et al., *New Constraints on the Faint End of the UV Luminosity Function at $z \sim 7-8$ Using the Gravitational Lensing of the Hubble Frontier Fields Cluster A2744*, ApJ **800** (2015), 18
- [57] Vale, A., Ostriker, J.P., *Linking halo mass to galaxy luminosity*, MNRAS **353** (2004), 189
- [58] Shankar, F., Lapi, A., Salucci, P., De Zotti, G., Danese, L., *New Relationships between Galaxy Properties and Host Halo Mass, and the Role of Feedbacks in Galaxy Formation*, ApJ **643** (2006), 14

- [59] Moster, B.P., Naab, T., White, S.D.M., *Galactic star formation and accretion histories from matching galaxies to dark matter haloes*, MNRAS **428** (2013), 3121
- [60] Aversa, R., Lapi, A., De Zotti, G., Danese, L., *Black Hole and Galaxy Coevolution from Continuity Equation and Abundance Matching*, ApJ, submitted
- [61] Finlator, K., Dav, R., Ozel, F., *Galactic Outflows and Photoionization Heating in the Reionization Epoch*, ApJ **743** (2011), 169
- [62] Weisz, D.R., Johnson, B.D., Conroy, C., *The Very Faint End of the UV Luminosity Function over Cosmic Time: Constraints from the Local Group Fossil Record*, ApJ **794**, L3
- [63] Boylan-Kolchin, M., Bullock, J.S., Garrison-Kimmel, S., *Near-field limits on the role of faint galaxies in cosmic reionization*, MNRAS **443** (2014), L44
- [64] Efstathiou, G., *Suppressing the formation of dwarf galaxies via photoionization*, MNRAS, **256** (1992), 43
- [65] Sobacchi, E., Mesinger, A., *How does radiative feedback from an ultraviolet background impact reionization?*, MNRAS **432** (2013), 3340
- [66] Cai, Z.-Y., et al., *A Physical Model for the Evolving Ultraviolet Luminosity Function of High Redshift Galaxies and their Contribution to the Cosmic Reionization*, ApJ, **785** (2014), 65
- [67] Duncan, K., et al., *The mass evolution of the first galaxies: stellar mass functions and star formation rates at $4 < z < 7$ in the CANDELS GOODS-South field*, MNRAS **444** (2014), 2960
- [68] Carilli, C.L. et al., *Square Kilometer Array key Science: a progressive retrospective*, PoS **AASKA14**, id. 171
- [69] Carucci, C.L. et al., *Warm dark matter signatures on the 21 cm power spectrum: intensity mapping forecasts for SKA*, JCAP, submitted, arXiv:150206961
- [70] Brooks, A., *Re-examining astrophysical constraints on the dark matter model*, AnP **526** (2014), 294

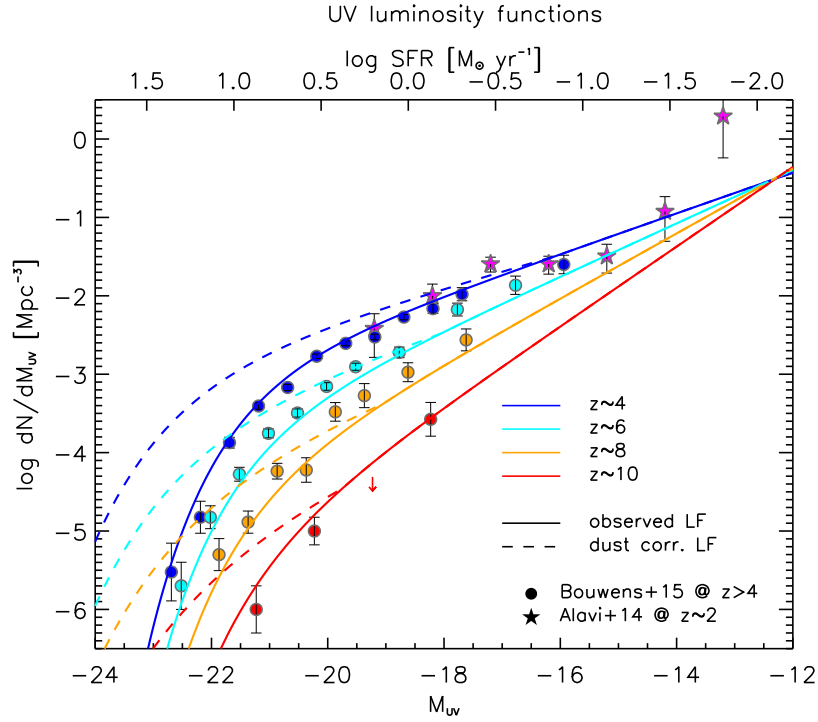


Figure 1. The UV luminosity function. Circles refer to data points from the *Hubble Space Telescope* [25] at $z \sim 4$ (blue), 6 (cyan), 8 (orange), and 10 (red), with the solid lines illustrating their analytic renditions in terms of Schechter functions; the dashed lines include dust-correction estimated from the UV continuum spectral slope [27]. The purple stars show the ultra-faint luminosity function at $z \sim 2$ measured with the aid of gravitational lensing by a foreground galaxy cluster [37]. The upper scale refers to the SFR associated with the dust-corrected UV magnitude.

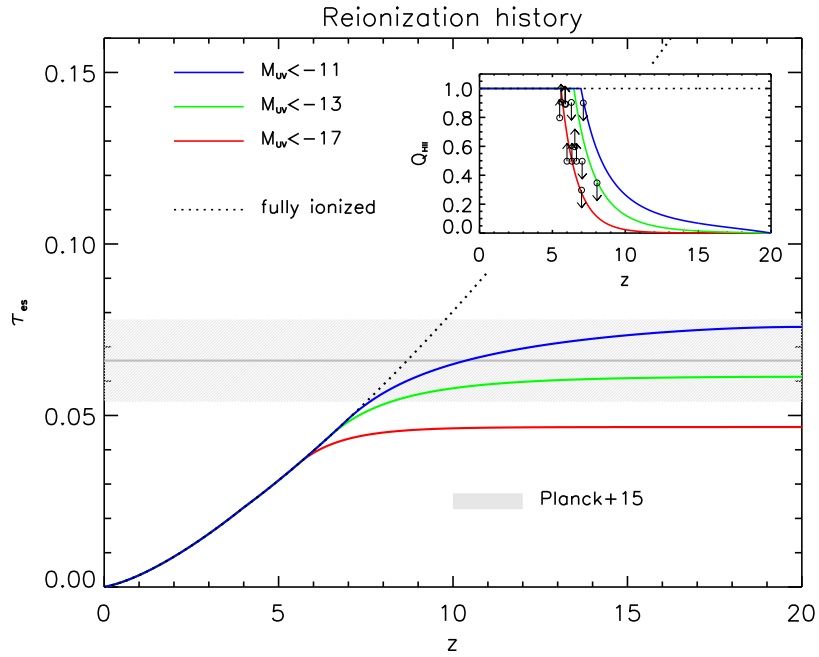


Figure 2. The evolution with redshift of the electron scattering optical depth τ_{es} . Solid lines illustrate the result by using the luminosity functions down to a limiting magnitude $M_{\text{UV}} = -17$ (red), -13 (green), and -11 (blue), see text. For reference, the black dotted line refers to a fully ionized Universe up to redshift z . The grey shaded area shows the measurement (with 1σ uncertainty region) from the *Planck* Collaboration [1]. In the inset, the corresponding evolution of the ionized fraction Q_{HII} is plotted, together with upper and lower limits from various observations [31].

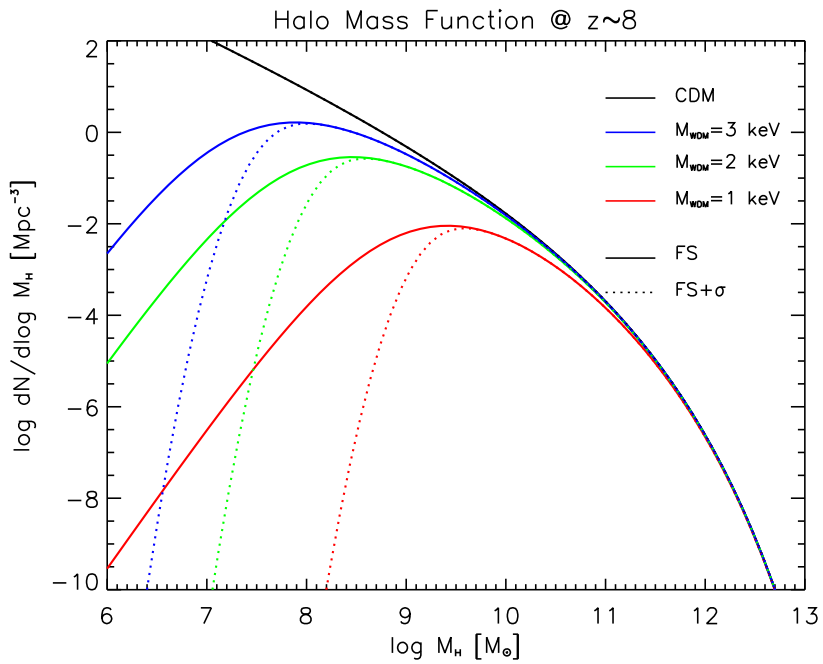


Figure 3. The halo mass function at $z \sim 8$, for different values of the WDM mass $M_{\text{WDM}} = 1$ (red), 2 (green), and 3 (blue) keV. The solid lines include only the free-streaming effect, while dotted lines also take into account the effective pressure from residual velocity dispersion of the WDM particles [16, 43]. For reference, the black solid line shows the halo mass function for standard CDM.

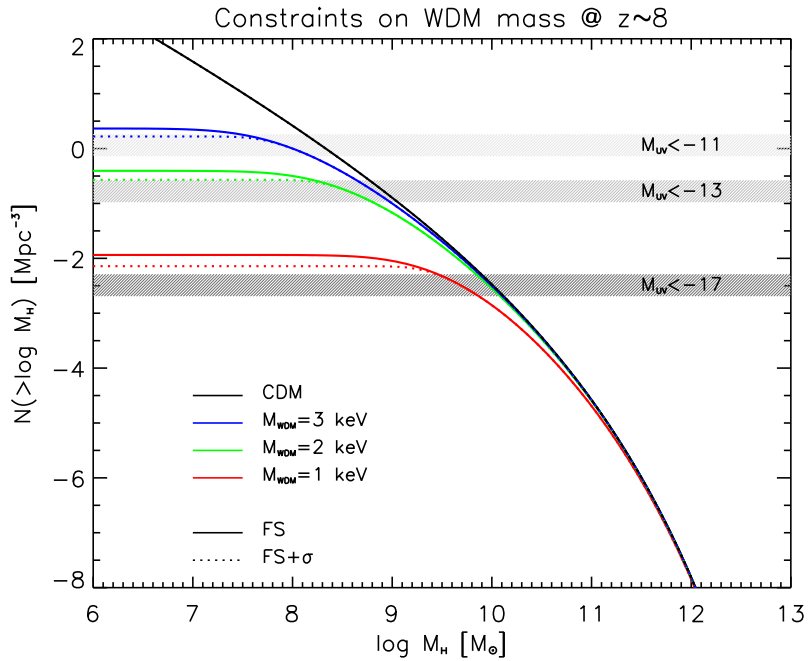


Figure 4. Constraints on the WDM mass at $z \sim 8$ in terms of the comparison between the integrated number density of halos and galaxies. The grey shaded areas represent the integrated number density of galaxies down to limiting magnitudes $M_{\text{UV}} = -17$, -13 , and -11 , as labeled. The lines refer to the integrated number density of halos, for different values of the WDM mass $M_{\text{WDM}} = 1$ (red), 2 (green), and 3 (blue) keV. The solid lines include only the free-streaming effect, while the dotted lines also take into account the effective pressure from the residual velocity dispersion of the WDM particles. For reference, the black solid line shows the outcome for standard CDM.

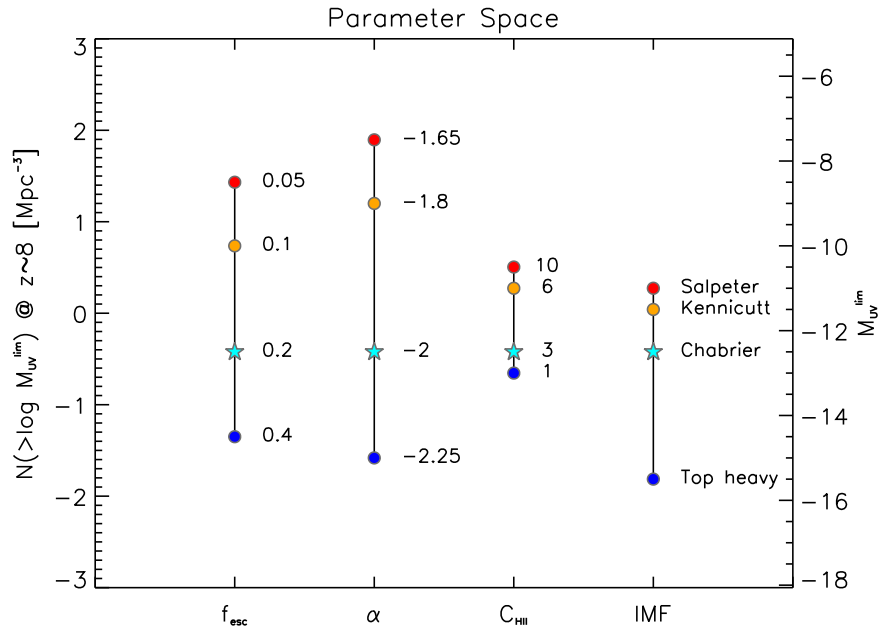


Figure 5. Effects on our results of varying the basic assumptions concerning: the escape fraction of ionizing photons f_{esc} , the faint-end slope of the UV luminosity function α , the clumping factor C_{HII} of the intergalactic medium, and the IMF. The right axis shows the limiting magnitude, and the left axis shows the corresponding integrated galaxy number density, required to match the *Planck* best fit of $\tau_{\text{es}} \approx 0.066$. Our fiducial values of the parameters are illustrated as cyan stars, while the dots represent larger and lower values as labeled.

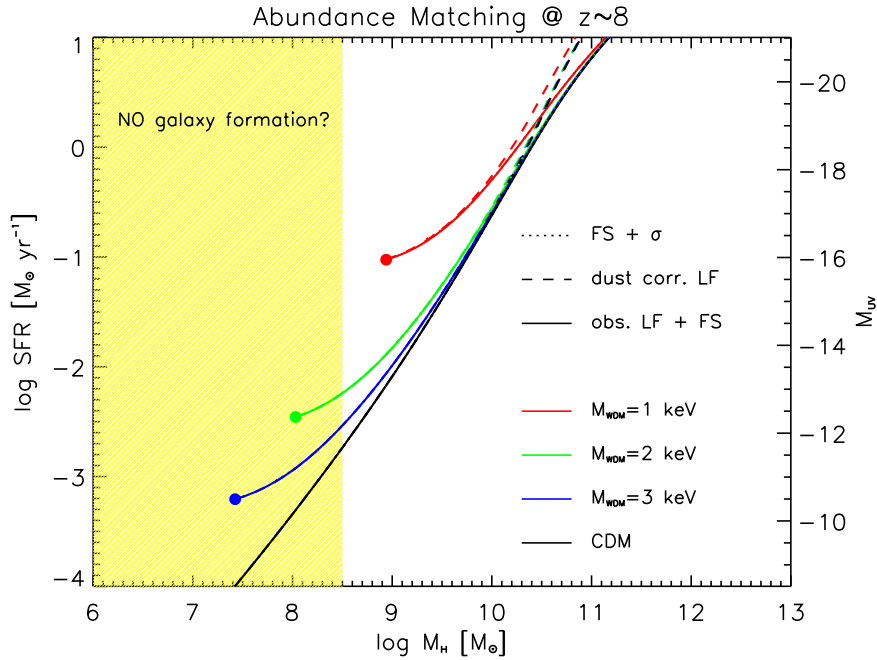


Figure 6. The UV magnitude (right axis) and the SFR (left axis) plotted against the halo mass at $z \sim 8$, obtained from the abundance matching technique, for different values of the WDM mass $M_{\text{WDM}} = 1$ (red), 2 (green), and 3 (blue) keV. The solid lines refer to the results obtained by using the observed galaxy luminosity functions and the halo mass functions with only free streaming effects included. The dashed lines were obtained using the dust-corrected galaxy luminosity functions, while the dotted lines (which turn out to be nearly coincident with the solid lines) were obtained from the halo mass functions with inclusion of both free-streaming and velocity dispersion effects. For reference, the black solid line shows the outcome for standard CDM. In WDM scenarios, the colored curves are interrupted at the free-streaming mass scale (indicated by a filled dot). The yellow shaded area marks the region where galaxy formation must be inefficient so as not to produce, according to observations and simulations [63], too many satellites in Milky Way-sized halos at $z \sim 0$.

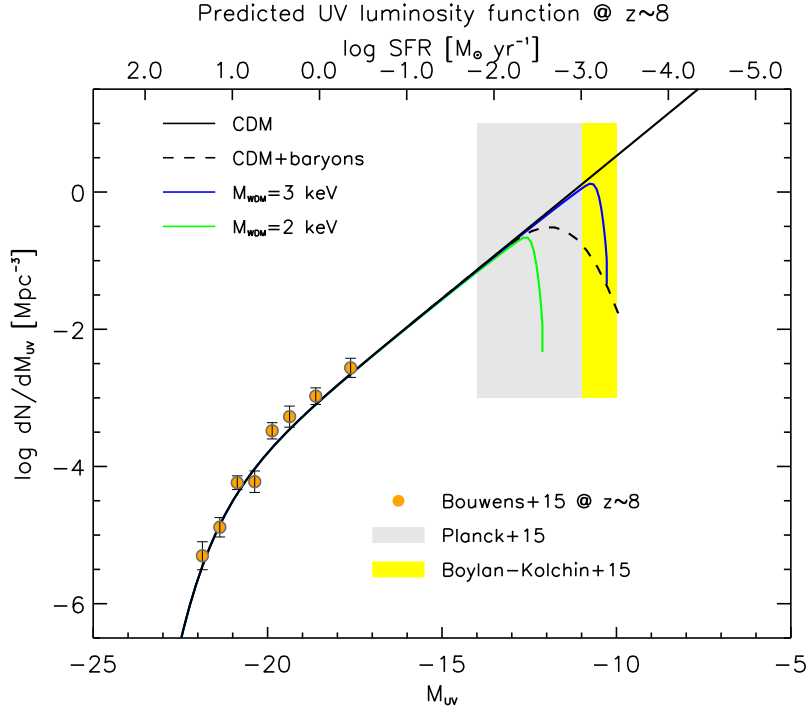


Figure 7. Predictions on the very faint end of the UV luminosity function at $z \sim 8$, obtained by combining the M_{UV} vs. M_H relationships of Fig. 6 with the halo mass function. Colored lines refer to different values of the WDM mass $M_{WDM} = 2$ (green) and 3 (blue) keV; solid black line is for pure CDM, while dashed black line includes baryonic effects (see text) required not to run into the missing satellite problem. Orange circles show the data at $z \sim 8$ [25]. The shaded areas illustrate the range of magnitudes where the luminosity function must downturn to be consistent with the reionization history of the Universe from *Planck* [1] data (grey shade; cf. Fig. 2) and not to run into the satellite problem (yellow shade; cf. Fig. 6).